Advanced Composite Materials
Publication details, including instructions for authors and subscription information:
http://www.tandfonline.com/loi/tacm20

Mechanical properties of knitted fabric reinforced polypropylene composites

N. K. Cuong , H. Yamane & Z. Maekawa

Version of record first published: 02 Apr 2012.

Adv. Composite Mater., Vol. 9, No. 1, pp. 25–35 (2000)

Mechanical properties of knitted fabric reinforced polypropylene composites

N. K. CUONG [1], H. YAMANE [2] and Z. MAEKAWA [2,*]

[1] *Department of Polymer Science and Engineering, Japan*
[2] *Division of Advanced Fibro-Science, Kyoto Institute of Technology, Sakyo-ku, Matsugasaki, Kyoto 606, Japan*

Received 16 September 1998; accepted 13 March 1999

Abstract—A study is conducted on the effects of cooling conditions on flexural properties of aramid fiber knitted fabric (AFKF) and glass fiber knitted fabric (GFKF) reinforced thermoplastic polypropylene composites. To study these effects, composite laminates are fabricated under a molding pressure of 3 MPa for 20 min, then consolidated from the melt at different cooling conditions: rapid cooling, i.e. quasi-quenching, and gradual cooling. Flexural tests are carried out on specimens in two directions: wale and course. Evaluation on thermal properties and morphology is studied using a differential scanning calorimetry (DSC). Flexural properties are little sensitive to the cooling rates; however, gradually cooled specimens show higher level of crystallinity than rapidly cooled specimens. Furthermore, flexural strengths display higher in the wale than in the course directions. SEM micrographs of fracture surfaces reveal poor adhesion between the fiber and polypropylene matrix.

Keywords: Knitted fabric composites; wale and course directions; rapid cooling; gradual cooling; crystallinity; flexural properties.

1. INTRODUCTION

Mechanical properties of semi-crystalline thermoplastic composites greatly depend on material processing conditions. Effects of cooling rates on crystallinity, morphology and mechanical properties of high performance semi-crystalline thermoplastic composites have been investigated in recent years [1–4]. However, most studies on thermoplastic composites have involved the use of unidirectional fiber yarns and rigid semi-crystalline polymers due to their high modulus and yield strength, such

*To whom correspondence should be addressed.

as semi-crystalline poly-ether-ether-ketone (PEEK), polyphenylene sulphide (PPS) and many others.

Composite materials based on polypropylene matrix resins (PP) reinforced with knitted fabrics that have large deformation and low modulus are suitable for membranous composite materials. Knitted fabrics with excellent drape-ability and net shape manufacture ability are finding applications in composite materials [5]. In recent years, many research works on mechanical properties of knitted fabric composites have been investigated but most of these studies have used composite materials based on epoxy resin [6–8]. Recently, Ramakrishna *et al.* [9, 10] have investigated the fabrication of glass fiber knitted fabric reinforced with polypropylene matrix composites. The effects of impregnation time and stitch densities on tensile properties of the knitted fabric composites have been identified.

In the work reported here, aramid fiber knitted fabric reinforced polypropylene (AFKF/PP) and glass fiber knitted fabric reinforced polypropylene (GFKF/PP) composites were fabricated by controlling consolidation conditions. The effects of the cooling conditions on flexural properties of AFKF/PP and GFKF/PP were studied. The degree of crystallinity of the PP matrix as well as fracture surfaces of the knitted fabric composite laminates were examined by using differential scanning calorimetry (DSC) and scanning electron microscope (SEM) respectively.

2. EXPERIMENTAL PROCEDURES

2.1. Materials

Aramid fiber yarns of 1140 denier (Kevlar 49, type 965) and glass fiber yarns (ECD 450 1/2 4-45Y-23) with $D_y = 1600$ denier were supplied by Toray Dupon Co. Ltd. and Nippon Electric Glass Co. Ltd. Japan, respectively. Two types of these yarns were used to produce plain knit fabrics. Unmodified polypropylene (PP) sheets of 0.5 mm in thickness obtained from Idemitsu NSG Co. Ltd. Japan were used as polymer matrix.

2.2. Knitted fabrics

The research work described in this paper is mainly concerned with a plain weft knitted fabric. An optical photograph and a schematic diagram of the knit fabric are illustrated in Fig. 1. The knitted fabric produced on a flat bed weft knitting machine with a single set of needles using aramid and glass fiber yarns consists of the row of knit loops in the width direction and the column of knit loops in the longitudinal direction of the fabric. Respective directions are called ‘course direction’ and ‘wale direction’. Knitted fabrics are often specified using stitch density (S.D.) that is defined as the total number of knitted loops per unit area of the fabric. In this study, the knitted fabric with a stitch density of 22 loops/cm^2 was produced.

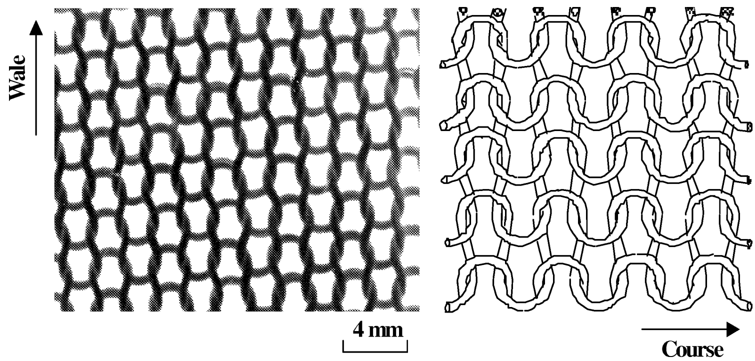

Figure 1. Optical photograph and schematic diagram of a glass fiber plain knit fabric.

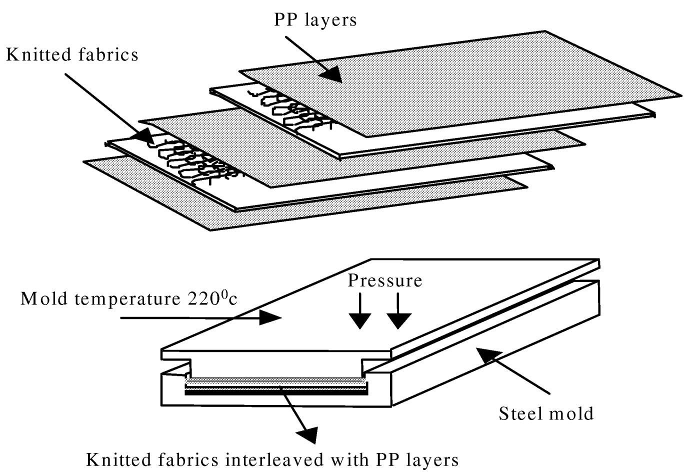

Figure 2. Schematic diagram for fabrication of knitted fabric composites.

2.3. Composite fabrication

Four plies of the knitted fabric aligned with respect to each other were stacked together with PP layers then placed into a mold. The mold (illustrated in Fig. 2) was first heated to 220°C; after reaching this molding temperature, a compressive pressure of 3 MPa was applied over a period of 20 min. Then, the mold was instantly immersed in a large volume of iced water (cooling rate: 140°C/min, Type-R) for the quasi-quenched specimens. The mold was also subjected to the same processing conditions for the gradually cooled specimens (Type-G) before cooling to the room temperature (RT) at a cooling rate of 5°C/min. Neat PP samples of 3 mm in thickness were also fabricated with the same processing conditions for the knitted fabric composites. Fiber volume fractions of AFKF/PP and GFKF/PP panels were determined by a specific gravity and a combustion method respectively.

2.4. Flexural tests

Three-point flexural tests were carried out with a support length (l) to thickness (h) ratio of $10:1$ as the composite laminates are rather flexible as a result of the effects of curved yarns of knitted fabrics and their low fiber volume fraction. The specimen geometry prepared by cutting parallel to the wale and course directions of the fabric was $10h + 20$ mm long, 25 mm wide and 3 mm thick, using a water-cooled rotary diamond saw. The experiment was repeated on a set of five specimens at room temperature using an Instron testing machine (Type-4206) at a cross-head rate of 1 mm/min. Fracture surfaces of the flexural specimens sputter-coated with a thin layer of gold were observed by using a scanning electron microscope (JEOL, model JSM-5200).

2.5. Differential Scanning Calorimetry (DSC)

The degree of crystallinity of the PP matrix in the neat PP samples as well as the knitted fabric laminates was assessed by using differential scanning calorimetry (DSC) carried out on a metric system of Perkin Elmer DSC7. A sample of 5 mg sealed in aluminum pans was heated to 220°C at the heating rate of 20°C/min and also crystallized at a cooling rate of 20°C/min. Thermal properties such as melting temperature, crystallization temperature and heat of diffusion were all determined from DSC thermograms. Experiments were conducted on three samples and their results were averaged. The degree of crystallinity of the composite was computed from the following expression:

$$X_c = \frac{\Delta H}{\Delta H^0\left(1 - \dfrac{V_f\rho_f}{V_f\rho_f + V_r\rho_r}\right)}100, \qquad (1)$$

where ΔH is the experimental heat of fusion, ΔH^0 is the heat of fusion of the complete crystalline PP ($\Delta H^0 = 190$ J/g [11]). V and ρ are the volume fraction and density; subscripts f and r refer to fiber and resin (aramid fiber: $\rho_f = 1.45$ g/cm^3, glass fiber: $\rho_f = 2.56$ g/cm^3 and polypropylene $\rho_r = 0.9$ g/cm^3 [12]). Fiber volume fractions of GFKF/PP and AFKF/PP are measured as 25% and 27% respectively.

3. RESULTS AND DISCUSSION

3.1. Relation between cooling conditions and thermal properties

Table 1 summarizes the thermal properties of GFKF/PP and AFKF/PP composites measured at the different cooling conditions. The melting temperature (T_m) and the crystallization temperature (T_c) of Type-R compared to those of Type-G are not considerably changed. It seems that different cooling rates have little or no effect on changes of these temperatures. The heat of fusion (ΔH) was lower in composites samples than in neat resins. This reduction was due to the lower fiber volume fraction as well as larger specific heat of neat PP samples than those of composite samples. There are clear differences in the degree of crystallinity, X_c, at the different cooling rates for neat PP matrix and matrix in composite materials; The degrees of crystallinity of the composite materials, however, indicate lower values than those of the neat PP polymer matrix. This may be attributed to the presence of fiber bundles (aramid or glass fibers) in composite materials. By observing PP morphologies produced by each cooling, it can be seen that morphologies of Type-R possessed transcrystallinity-like kink bands in the fiber vicinity, whereas Type-G was wholly spherulitic even along the embedded fiber bundles [13]; also, in Type-G, the size of spherulites was smaller in the vicinity of fiber bundles than in resin-rich regions [14]. Therefore, it could be said that the cooling conditions as well as fiber bundles had little effects on the degree of crystallinity of PP polymer matrix in composite materials.

3.2. Flexural properties

The typical flexural stress–deflection curves of Type-R and Type-G for GFKF/PP composites in the wale direction are shown in Fig. 3. When the deflection was small, the flexural stresses of Type-G seem to be slightly higher in comparison with that of Type-R. With further deflection, stress values of Type-G were inverse; they were lower than values of Type-R. Higher failure stresses and deflections of Type-R may be attributed to a higher degree of crystallinity in rapid cooling. The same tendency of the Type-R and the Type-G was also obtained for AFKF/PP composites. Flexural strengths of AFKF/PP and GFKF/PP composites are presented in Fig. 4. It can be seen that the flexural strengths of both the wale and course specimens were slightly affected by the cooling rates. Flexural strengths of type-R were higher than those of Type-G. The enhancement of flexural strengths of Type-R may be attributed to two possible reasons: one is improvement of properties of the matrix

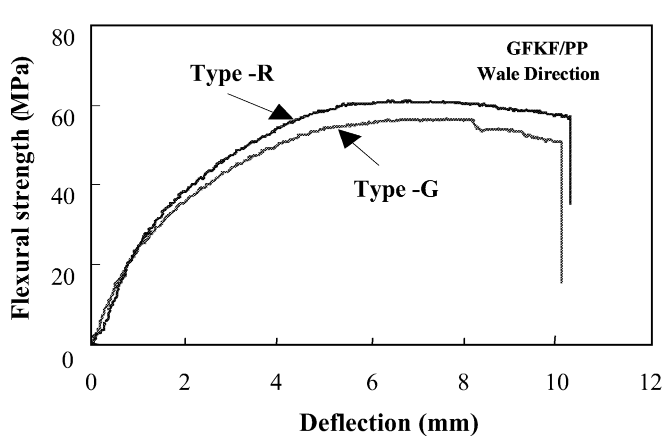

Figure 3. Typical flexural stress-deflection curves of GFKF/PP at different cooling conditions.

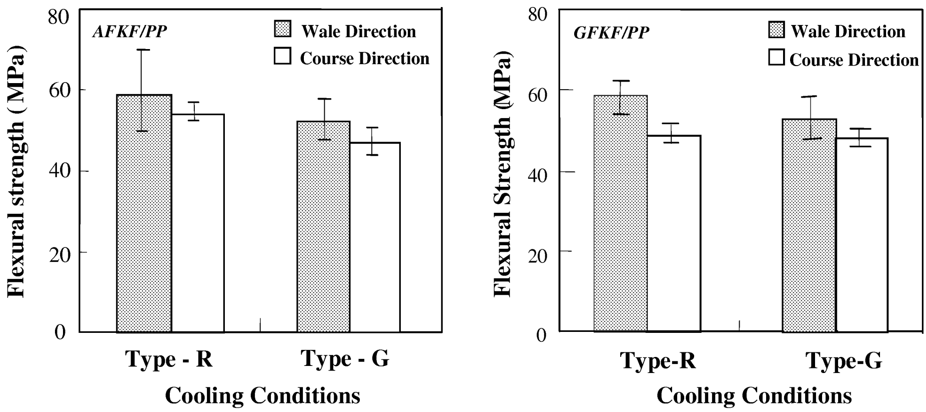

Figure 4. Flexural strengths of AFKF/PP and GFKF/PP composites *versus* different cooling conditions.

Table 1.
Thermal properties of the composites at different cooling conditions

Samples type	Near PP		GFKF/PP		AFKF/PP	
	R	G	R	G	R	G
T_m (°C)	161.1	161.2	160.8	161.3	161.9	160.4
T_c (°C)	102.7	101.5	101.3	101.7	101.7	101.7
ΔH (J/g)	65.5	84.0	29.8	33.9	34.5	38.5
X_c (%)	34.4	44.2	30.6	34.3	29.0	32.4

itself and the other is a change of interfacial strength between fiber and matrix. The improvement of properties comes from the matrix itself due to changes in the degree of crystallinity or spherulite morphology. The slightly increasing the degree of crystallinity for Type-R compared with Type-G is displayed in Table 1. Another possibility is the improvement of interfacial strength between fiber and matrix. This is attributed to the higher amorphous contents of Type-R resulted in the larger wetted fiber surface area due to smaller spherulite size which made an increase in the fiber/matrix adhesive quality. It has also been proved by Hocker *et al.* [15], where they studied the effect of crystallinity on the fiber/matrix adhesion in single glass-fiber/PP composites at rapid (Type-R) and gradual cooling (Type-G) conditions. The interfacial shear strength of Type-R for pulling out a single fiber embedded in a flat block PP matrix that was higher than that of Type-G have been reported. Also, both the Type-R and Type-G specimens display higher flexural strengths in the wale direction than in the course direction. It might be that the higher proportion of fiber bundles of the knitted fabric was oriented in the wale than in the course direction.

Showing a different tendency to the flexural strength, in Fig. 5, values of flexural moduli of Type-R for both the wale and course specimens were lower than those of

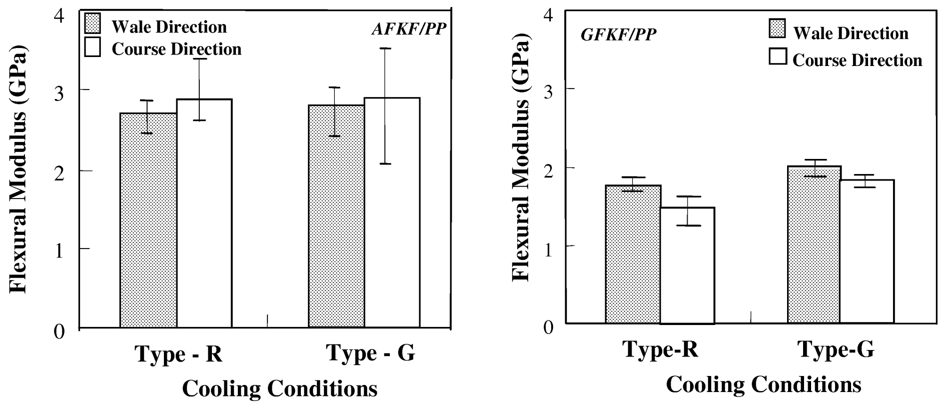

Figure 5. Flexural moduli of AFKF/PP and GFKF/PP composites *versus* different cooling conditions.

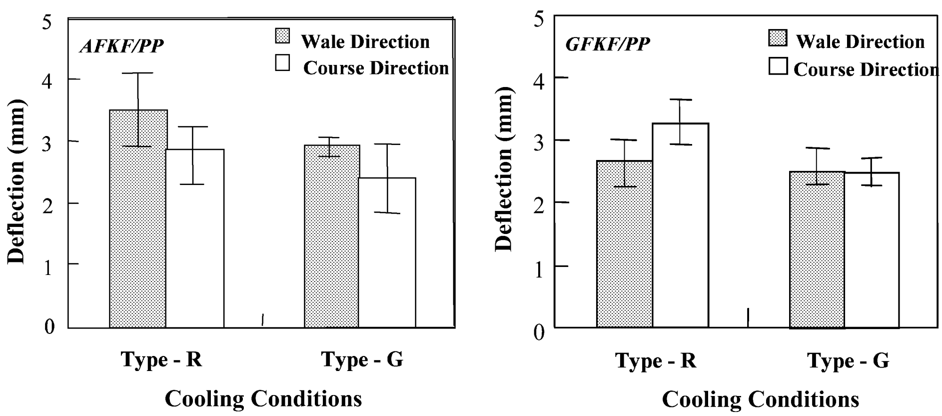

Figure 6. Deflections of AFKF/PP and GFKF/PP composites *versus* different cooling conditions.

Type-G. Besides, higher deflections of Type-R in comparison with deflections of Type-G are demonstrated in Fig. 6. It seems that the matrix of type-R was more ductile than that of Type-G. Thus, flexural moduli of the composites were sensitive to the cooling rates. This might be attributed to the effect of reducing the degree of crystallinity of Type-R in the polymer matrix, i.e. the lower degree of crystallinity, the smaller spherulite size and the lower flexural modulus of Type-R.

SEM micrographs of fracture surfaces on the tensile side of AFKF/PP and GFKF/PP composites at the different cooling conditions, i.e. Type-R and Type-G, are shown in Fig. 7a, Fig. 7b and Fig. 8a, Fig. 8b respectively. It can be seen that matrix fracture of both composites at resin rich regions occurred in various ways. Matrix of Type-R failed in the typical ductile manner, while matrix of Type-G displayed weak bonding due to failure edges that appeared to be relatively smooth. The ductility of Type-R is illustrated by plastic deformation of PP matrix

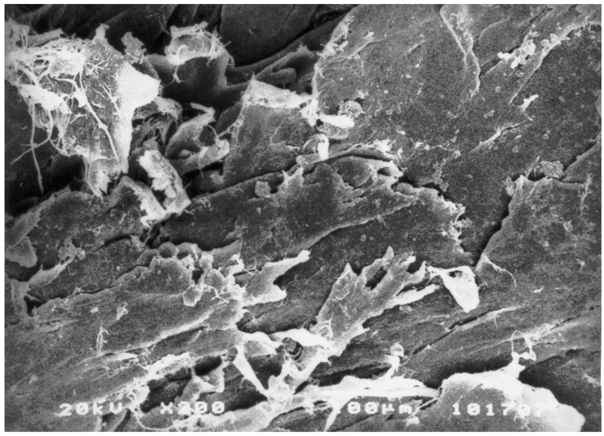

(a) Type-R, AFKF/PP composites. 100 μm

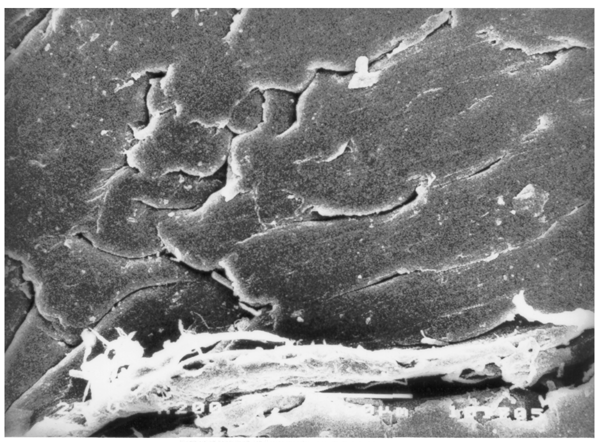

(b) Type-G, AFKF/PP composites. 100 μm

Figure 7. SEM micrographs of fracture surfaces of AFKF/PP composites for both Type-R and Type-G on tensile side. (a) Type-R, AFKF/PP composites. (b) Type-G, AFKF/PP composites.

pulled out in the form of small hills (Fig. 7a, Fig. 8a). Its fracture surface looks rather coarse whereas the fracture surface of Type-G seems to be relatively smooth and on macroscopic scale, without any significant matrix deformation (Fig. 7b, Fig. 8b).

Fiber surfaces in both cases, rapid and gradual cooling conditions of both composites, were also observed by using SEM. Some small pieces of matrix resin like small heaps were attached the fiber surfaces of Type-R of AFKF/PP composites (shown in Fig. 9a) whereas the fiber surfaces of Type-G looks rather clean and smooth (Fig. 9b) as no matrix pieces were to be seen on its fiber surfaces. Hence,

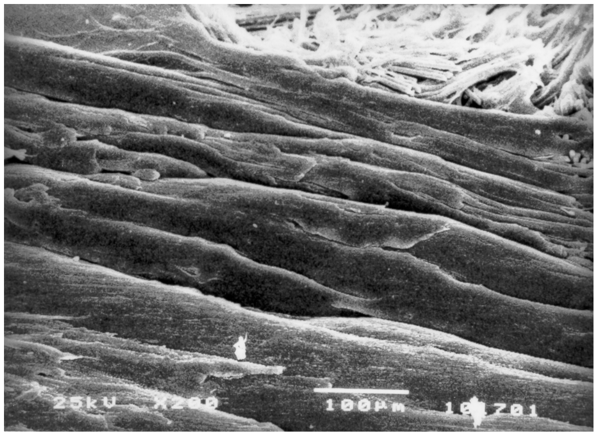

(a) Type-R, GFKF/PP composites.

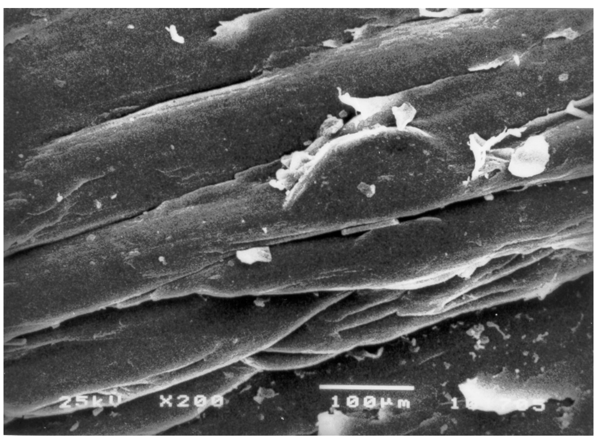

(b) Type-G, GFKF/PP composites.

Figure 8. SEM micrographs of fracture surfaces of GFKF/PP composites for both Type-R and Type-G on tensile side. (a) Type-R, GFKF/PP composites. (b) Type-G, GFKF/PP composites.

little or non-retention of the matrix on the fiber surfaces shows the poor adhesion between fiber and matrix especially between aramid fiber and matrix resins.

4. CONCLUSIONS

The results described above have shown the effects of the cooling conditions on flexural properties of aramid fiber and glass fiber knitted fabric reinforced thermoplastic polypropylene composites (AFKF/PP and GFKF/PP). The cooling conditions have a little effect on flexural properties. The thermal properties indicate

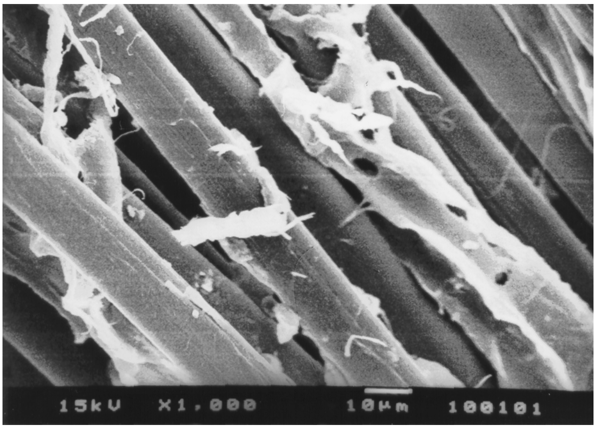

(a) Type-R

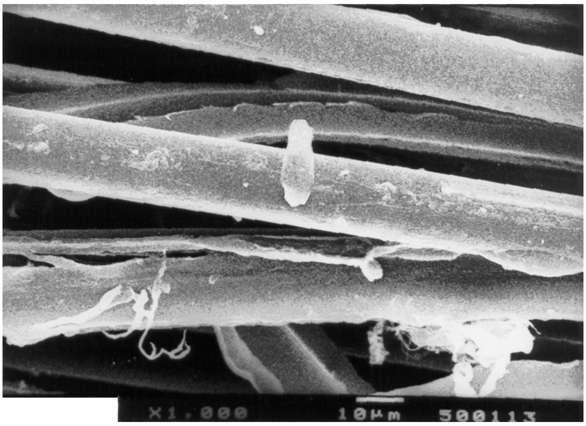

(b) Type-G

Figure 9. SEM micrographs of fracture surfaces showing fiber/matrix adhesion of AFKF/PP, (a) Type-R, (b) Type-G.

that the melting temperature and the crystallization temperature of the matrix resins are not affected by cooling conditions. Crystallinity is lower in rapid cooling than gradual cooling and the flexural properties are little sensitive to the level of crystallinity in the matrix resin. SEM micrographs of the fracture surfaces reveal poor fiber/matrix adhesion.

REFERENCES

1. P. Vautey, Cooling rate effects on the mechanical properties of a semi-crystalline thermoplastic composite, *SAMPE Quart.* **21**, 23–28 (1990).
2. W. J. Cantwell *et al.*, The effect of cooling rate on deformation and fracture in IM6/PEEK composites, *Comp. Struct.* **14**, 151–171 (1990).

3. L. Ye, A. Beehag and K. Friedrich, Mesostructural aspects of interlaminar fracture in thermoplastic composites: is crystalline a key? *Comp. Sci. Technol.* **53**, 167–173 (1995).
4. A. Beehag and L. Ye, Role of cooling pressure on interlaminar fracture properties of commingled CF/PEEK composites, *Composites, Part A* **27A**, 175–182 (1996).
5. J. Mayer, K. Ruffieux, R. Tognini and E. Wintermantel, Knitted carbon fibers, a sophisticated textile reinforcement that offers new perspectives in thermoplastic composite processing, in: *Proc. of ECCM6*, A. R. Bunsell, A. Kelly and A. Massiah (Eds), pp. 219–224. Woodhead Publishing Limited, Bordeaux (1993).
6. S. Ramakrishna, A. Fujita, N. K. Cuong and H. Hamada, Tensile Failure Mechanisms of Knitted Glass Fiber Fabric Reinforced Epoxy Composites, in: *Proc. of 4th Japan International SAMPE Symposium & Exhibition*, Z. Maekawa, E. Nakata and Y. Sakatani (Eds), Vol. I, pp. 661–666. Tokyo (1995).
7. D. Phillips and I. Verpoest, Sandwich panels produced from 3D-knitted structures, in: *Proc. of 40th International SAMPE Symposium*, pp. 957–965. Anaheim, California (1995).
8. F. K. Ko, C. M. Pastore, J. M. Yang and T. W. Chou, Structure and properties of multilayer multidirectional warp knit fabric reinforced composites, in: *Composites '86: Recent Advances in Japan and The United States*, K. Kawata, S. Umekawa and A. Kobayashi (Eds), pp. 21–28. Japan Society for Composite Materials, Tokyo (1986).
9. S. Ramakrishna, H. Hamada and N. K. Cuong, Fabrication of knitted glass fiber fabric reinforced thermoplastic composite laminates, *J. Adv. Comp. Let.* **3**, 189–192 (1994).
10. S. Ramakrishna, H. Hamada, N. K. Cuong and Z. Maekawa, Mechanical properties of knitted fabric reinforced thermoplastic composites, in: *In Proc. of ICCM-10*, A. Poursartip and K. Street (Eds), Vol. IV, pp. 245–252. Woodhead Publishing Limited, Vancouver (1995).
11. Service instructions, TA-4000 thermal analysis, measurement and evaluation system, Version 6.7, Mettler Instrument AG, GH-8606 Greifensee, Switzerland (1990).
12. D. Hull, in: *An Introduction to Composite Materials*, pp. 14–33. Cambridge University Press, Cambridge, UK (1981).
13. H. M. Butler, D. J. Bannister and R. J. Young, A study of transcrystalline polypropylene/single–aramid–fiber pull-out behavior using Raman spectroscopy, *Composites, Part A* **27A**, 833–838 (1996).
14. L. Ye and K. Friedrich, Mode I interlaminar fracture of co-mingled yarn based glass/polypropylene composites, *Compos. Sci. Technol.* **46**, 187–198 (1993).
15. F. Hoecker and J. Karger-Kocsis, Effects of matrix microstructure on interfacial strength in GF/PP examined by a single fiber pull-out technique, *Mechanics Compos. Mater.* **29**, 723–733 (1993).